iJRASET
International Journal For Research in
Applied Science and Engineering Technology

INTERNATIONAL JOURNAL FOR RESEARCH
IN APPLIED SCIENCE & ENGINEERING TECHNOLOGY

Volume: 4 Issue: IX Month of publication: September 2016

DOI:

A Research Paper on Optimum Energy in Household Refrigeration Cooling Systems

Shivendra Singh[1], Satish Singh[2]
[1]*M.Tech Scholor –M Tech Engg. Department , Gargi Ins. Of Technology Bhopal*
[2]*Astt. Professor M Tech. Engg Department, VIST Bhopal*

Abstract--This thesis aims to produce comprehensive methodology for testing, modeling, performance analysis and optimization for small capacity absorption chillers. The data for chilled water, cooling water and hot water develops deferent mathematical models for small capacity absorption machine. These models can further use testing and optimizing operation of absorption machine in air-conditioning systems. The methods used in this thesis are derived from experimental work and building energy system design. In order to achieve this aim, the following were defined: Comprehensive literature review is performed on absorption technology and standards including small capacity absorption machines and their integration into solar-assisted air-conditioning systems. Developing strategies for design and selection of proper air-conditioning in buildings capable of providing safe, healthier, productive and comfortable working environment to occupants. This is achieved by calculating cooling load of lift motor room by cooling load temperature deference method and radiant time series method. Develop various steady-state models based on experimental results using both physical and empirical approaches by thermodynamic modeling for the system.
KeyWords--Refrigerator , ANSYS, Evaporator

I. INTRODUCTION

The proliferation of energy consumption and carbon dioxide emissions in the built environment has made energy efficiency and savings strategies a priority objective for energy policies in most countries.Inrecent years particularly relevant has been the growth of energy consumption in HVAC systems,especially for cooling. Hence, the growing interest for the exploitation of renewable energy sources to meet the building thermal loads. Solar cooling is particularly promising to reduce electricity consumption in summer due to air conditioning, allowing alleviating the problem of electrical brownout or power blackout due to peak loads in hot summer days. Closed-cycle thermally driven absorption chillers are proven technology among the commercially available options [1,2].In the last decade, many researchers investigated the mutual interaction of the main components in a solar cooling system (solar collector field, storage tank, absorption chiller): the analysis and optimization of single components and of the whole system are typically carried out with a simulation software able to predict the performance under variable operating conditions [3,4].

II. LITERATURE REVIEW

Manuel Riepl et al.2012 Solar thermal cooling and heating plants with single-effect sorption chillers/ heat pumps promise primary energy savings compared to electric vapor compression chiller systems. M. Morsy El-Gohary [2013] This paper presents a co-generation system based on combined heat and power for commercial units. BoonritPrasartkaew [2014]This paper presents an experimental investigation on the performance of a small size absorption chiller which was renovated or developed from an old out-of-order commercial chiller. Martin Helm1 et al. [2014] A reliable solar thermal cooling and heating system with high solar fraction and seasonal energy efficiency ratio (SEER) is preferable. By now, bulky sensible buffer tanks are used to improve the solar fraction for heating purposes. Chougui Mohamed et al. [2014] The objective of this study is related to an absorption refrigeration system operating in an industrial manufacturing of detergent(Henkel Algeria). Roland Winstona et al.[2014]A solar thermal cooling system using novel non-tracking External Compound Parabolic Concentrators (XCPC) has been built and operated for two cooling seasons (summers of 2011 and 2012). Its performance in providing power for space cooling has-been analyzed. Roland Winstona et al. [2014]A solar thermal cooling system using novel non-tracking External Compound Parabolic Concentrators (XCPC) has been built and operated for two cooling seasons (summers of 2011 and 2012). HaiQuanSuna et al. [2015]Absorption cooling technologies have been researched for many years.Jeremy P. Osbornea et al. [2015]The University of Technology, Sydney (UTS) has built a unique tri-generation system that provides chilled water, hot water, and electricity to their new Faculty of Engineering and Information Technology (FEIT) building. Hang Yina, et al. [2015] To elucidate the energy-saving effect of pumps along with the heat-transfer performance of terminal units in heat pump systems, a comprehensive analysis of an assumed chilled-water circuit at two supply water temperatures under four variable-flow control modes was carried out from the viewpoint of available energy, i.e., energy. Subsequently, based on the operating data, the energy analysis of a heat pump system was carried out to verify the energy-saving effect after variable-frequency transformation of the chilled water pump.Giuseppe Franchinia et al. [2015]. In last decades, much effort has been made to drive cooling cycles exploiting renewable energy sources.

Simulation of Household refrigerators

Introduction

Model CHECKS

A. *Model Integrity Check*

The integrity is the consistency of the computer simulation and the governing equations. The model error is non-zero for several reasons:

1) Integration errors;
2) Linearity assumption, second order terms are usually neglected;
3) Discretization of the partial differential correlation with finite differences.
4) Round-off.

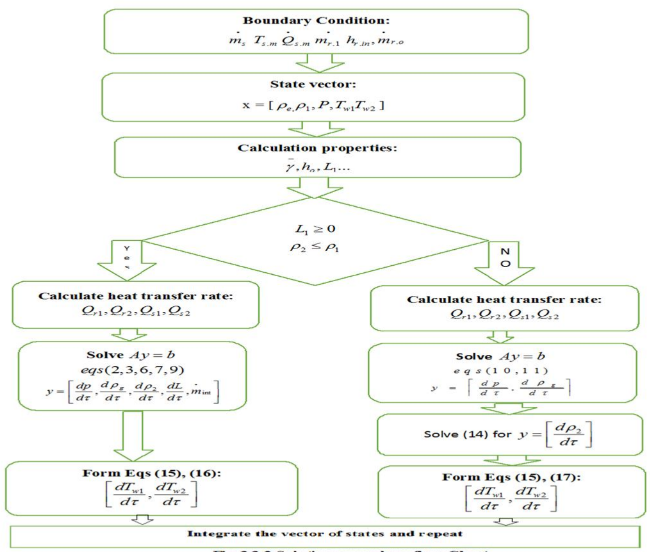

Fig.3.3.2 Solution procedure flow Chart

The model integrity was checked looking at the consistency of the simulation results with the integral forms of the continuity and energy equation. Several test cases are presented in thefollowingThe model was excited with different waveforms, comparing the mass and internal energy of the model to the values calculated with the integral forms. Analytic development the integrity check method is presented in Appendix. Table 3.2.1summarize tests results, which includes both TP and TP-V model simulations. Peak-topeakamplitudes and errors were expressed as percentage of the initial values. Recorded errors were always less than 0.0085%.

B. *State Variable Choice*

Rasmussen and Alleyne [35] underlined that the redundant nature of thermodynamic properties results in the possibility of expanding mass and energy equation with freedom in choosing the state variables. The complete derivation for the gas cooler for three different choices of refrigerant state variables was presented, namely 1) pressure and outlet enthalpy, 2) pressure and mass, 3) zone enthalpy andmass. The second and the third state representations are intrinsically mass conservative since they contain a pure integrator associated with the accumulation of refrigerant mass. The authors also found that for model reduction purposes these are the best choices. In this paper model the second state representation was adopted and fitted to the multiple modeling framework considering evaporator pressure, *p*, and mean density, eρ, as the refrigerant state variables together with average density, 2ρ , for the superheated zone characterization. A fully (mass and energy) conservative derivation is also possible if refrigerant pressure is replaced with the evaporator internal energy, *u*, inEq. (1). In this case the two-phase zone length can not be determined straightforwardly by Eq. (4) and algebraic manipulation is required. In the published approaches for the evaporator, two different groups of state variables were adopted, namely 1) pressure, outlet enthalpy and two-phase zone length(Pettit *et al.* [3]; 1998, Zhang and Zhang [30], 2006; Bendapudi*et al.* [19] and 2)pressure, mean void fraction and superheated zone enthalpy and two-phase zone length(Li and Alleyne [33]. As discussed in Section 3.2.4.2.2, Li and Alleyne [33] added an auxiliary equation determining mean void fraction time derivative. The resulting mass and energy state equation for one-zone model for thetwo approaches are reported in Appendix. Both the approaches are not intrinsically mass and energy conservative if the approximation errors associated to the expansion of the governing equations are considered. This could be critical when simulating evaporator's start-up from low mean void fraction considering the strong dependence of void fraction from quality. This would force to considerably reduce the minimum acceptable integration time step size. Besides this consideration a proper choice should be done for the simulation of particular conditions, such as the evaporator dynamic behaviorwith very low void fraction mean (γ). This is a typical working condition of refrigeration systems such as domestic refrigerators which require pressure equalization before compressor start up. During off periods most of the refrigerant charge flows to the evaporator, resulting in a very low mean void fraction at compressor start-up. Here a comparison between this model and the cited models is reported considering initial condition characterized by a very low mean void fraction (0.21), compressor start-up and no inlet mass flow rate. Table 3.2.3 summarizes the considered system geometry. In the solution system $Ay = b$, the b vector was set to a fixed value b = [-0.25; -51500].Figures 3.2.4 and 3.2.5 shows the mass and energy conservation errors (normalized to the mass and energy fluxes) after a single simulation time step as a function of the simulation time step length ranging from 0.01 to 10 s. In the Figure, the paper model is referred as "p-ρe", model 1) as "p-ho" while model 2) as "p-γ". As it can be pointed out, for all the models considered, conservation errors correctly tend to zero as the time step approaches zero. Clearly the mass conservation error for "p-ρe" is zero being the model intrinsically mass conservative. However "p-γ" model shows good performance, the mass conservation error ranging from 2.36 10-7 to 0.228% for 0.01 and 10 respectively. Instead model "p-ho" appears strongly affected by expansion errors as the simulation time steps increases, the mass conservation error ranging from 4.39 10-5 to12.1% for 0.01 and 10 s respectively. Simulations of 20 s period were carried out for four different constant integration time steps (0.01-0.1-1-10 s) considering both Zivi [38] (1964) and the homogeneousvoid fraction models. Table 3.2.2 summarizes the results at the end of the simulation in terms of mass and energy conservation errors (normalized to the initial values), pressure, mean void fraction and outlet enthalpy. In Figure 3.2.6 dew-point temperature and outlet quality trend for 1 s time step andZivi model are plotted. From Table 3.2.2 results it can be again pointed out thatthe paper model "p-ρe" and "p-γ" model show similar performance while "p-ho" modelappears strongly affected by expansion errors as the simulation time steps increases. AdoptingZivi void fraction model , the "p-γ" model mass conservation error ranges from -1.06 10-3 to -0.640%, while "p-ho" from -5.95 10-2 to 25.8% for 0.01 and10 s time step respectively. It can be concluded that models adopting state variables positioned on the evaporator geometrical boundaries seem critical from the mass and energy conservation point of view. Intrinsically conservative models or representations adopting averaged core state variables (such as the "p-γ" with the mean void fraction) appears the best suited for simulating very low mean void fraction conditions at compressor start-up.

C. Model Stability Check

The numerical stability of the model was checked with a test case simulation, holding constants the air and refrigerant inlet conditions and varying the refrigerant outlet mass flow rate with a sinusoidal shape trend. Thus leads to force repeated switching between representation schemes. Table 3.2.3 summarizes the physical parameters, initial and boundary conditions for the test case. As is it possible to see from fig. 3.2.7, the model simulation presents stiff transitions and smooth shaped outputs. Figure 3.2.9 reports integrity errors of the mass and of the refrigerant and wall internal energy. After a thousand seconds of simulation, the errors results less than0.13%. This result confirms the model integrity under repeated switching between schemes.

D. Model Validation

The moving boundary model was compared to one-dimensional finite volume evaporator model, which was developed and presented byBeghi and Cecchinato [14].

III. RESULTS AND DISCUSSION

In this chapter, variations of average energy consumption with year,Heat transfer Coefficients at evaporator Different Location,Air and Surface Temperature with distance from wall, Flow calculate, Pressure drop along the refrigerant tube at different mass fluxes, Pressure drop along the refrigerant tube at different mass fluxes and Single phase comparison of friction factor calculated. Given test condition. The object are all considered boundary conditions.

Test condition

S.N	T_1	T_2	mass flow in $\dot{m}$ (kg/s)	Mass flux G (kg/m^2s)[3]	Inlet vapor quality x (-)[4]	cooling capacity $\dot{Q}$ (w)[5]
1	-23.1	39.5	0.281	20.34	0.136	94.1
2	-19.7	41.8	0.331	24.03	0.134	111
3	-14	45.3	0.428	31.1	0.126	143
4	-9.3	48.5	0.519	37.67	0.127	172.2
5	-4.3	51.9	0.627	45.5	0.132	205.3

Show the energy consumption of household refrigerators, freezers and combinations in Sweden 1980-2000. As can be seen, the reduction is significant over the period. For the refrigerator is more than 30 percent. For the freezers and combinations the reduction is about 50 percent.

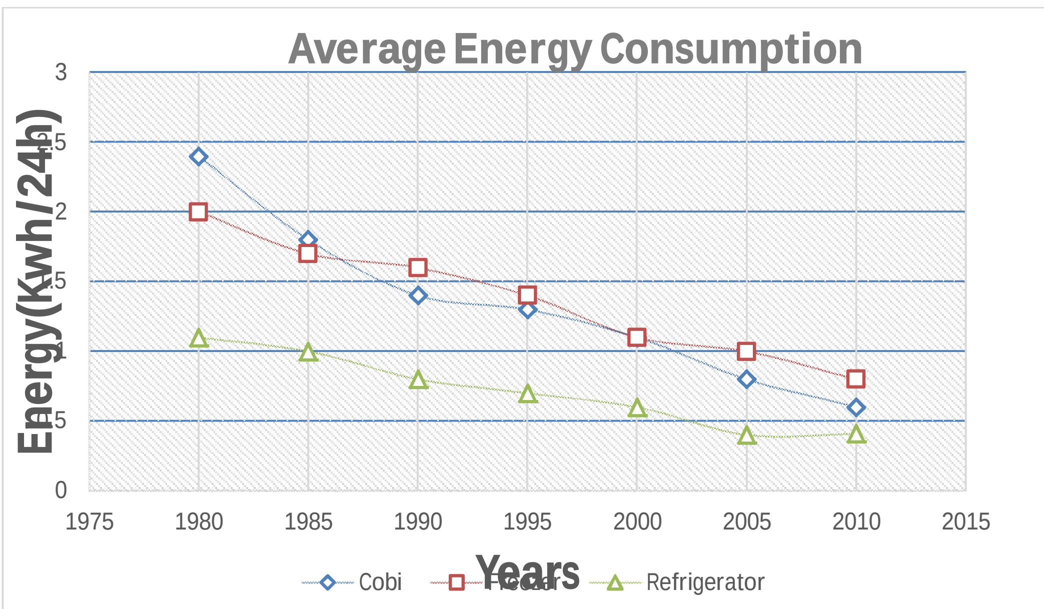

Fig.

Shows that the highest heat transfer coefficient (about 8.8 W/m² K) was observed when theevaporateas located in the cabinet's centre. When the evaporator was in its original location (wall location), the heat transfer coefficient decreased to about 7.6 W/m² K. When the air duct behind the evaporator was blocked the heat transfer coefficient decreased to about 5.1 W/m² K (both sides of evaporator used as calculated area in all cases). The figure also shows the estimated heat transfer coefficients (marked "theory" in the plot) whichh are the sum of the estimated free convection heat transfer and the estimated thermal radiation heat transfer. In all cases conventional black body radiation equations were used. For the centre located evaporator the Churchill and Chu correlation (Incropera and DeWitt, 1996) was used to estimate the free convection heat transfer. As can be seen, the estimated results are in good agreement with the experimental results. For the wall located evaporator, the free convection heat transfer of the evaporator front and back side was estimated in different ways to reflect the different flow

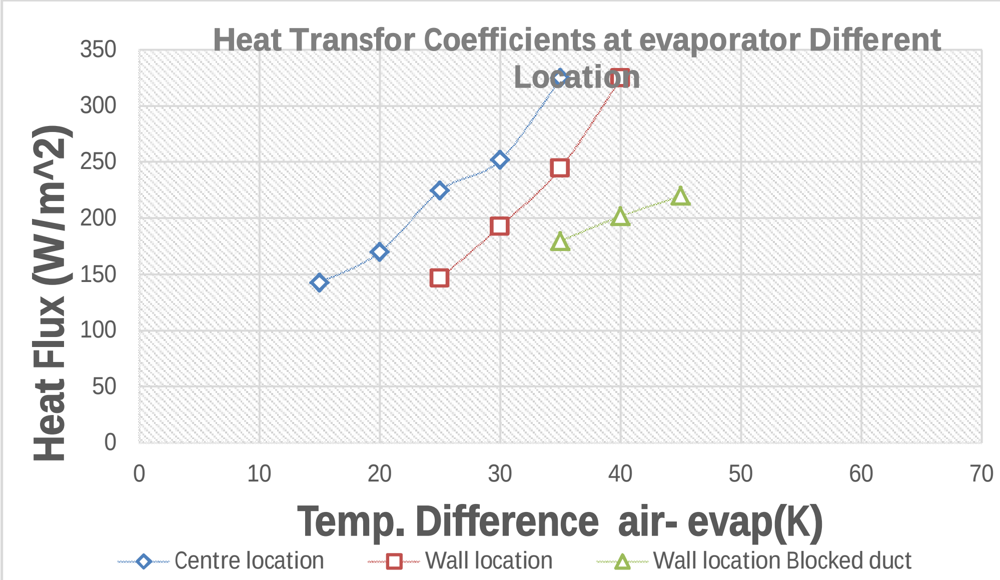

Fig . Heat transfer coefficients for different evaporator location

The evaporation temperature was in this measurement 15 °C, but due to thermal contact resistance the probe measured a few degree s higher temperatures at the evaporator surface. Above the evaporator (670 mm) the temperatures are almost constant at about 12 °C and thus "undisturbed" by the evaporator. On the evaporator outside, (i.e. distance from wall >25 mm) the other temperatures asym ptotically approach 10 °C, which was the approximate temperature in the cabinet.

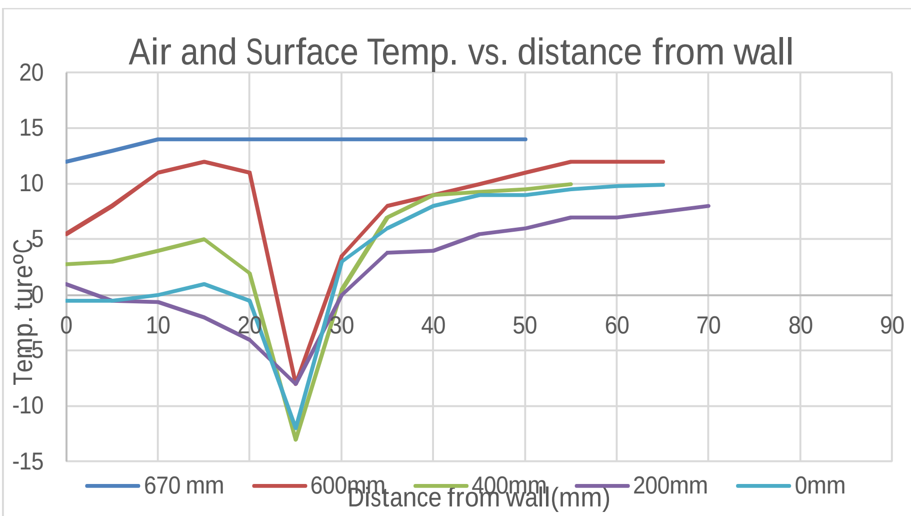

Fig Pressure drop along the refrigerant tube at different mass fluxes

Thermal boundary layers may be interpreted in the diagram at both sides of the evaporator, with increasing thickness at lower elevat ions. This is in agreement with classical boundary layer theory. In the duct behind the evaporator (i.e. distance from wall <25 mm) o ne can see that the wall, behind the evaporator (distance from wall 0 mm), is slightly colder than the air, which shows that this wall i s cooled by radiation exchange with the evaporator. This means that the air in the duct behind the evaporator is cooled by convectio n from both the evaporator and the wall.

It is seen that the flow is predicted to be wavystratified (solid line with small circles) for the mass flux 33 kg/m2s. For the lowest ma ss flux tested (21 kg/m2s) the flow was predicted to be stratified, and for the highest mass flux (43 kg/m2s) the flow was predicted t o be wavy-stratified. This means incomplete tube wetting in all cases. The liquid flows at the bottom of the refrigerant tube and the vapour at the top. However, these maps were developed for long, straight and circular tubes.

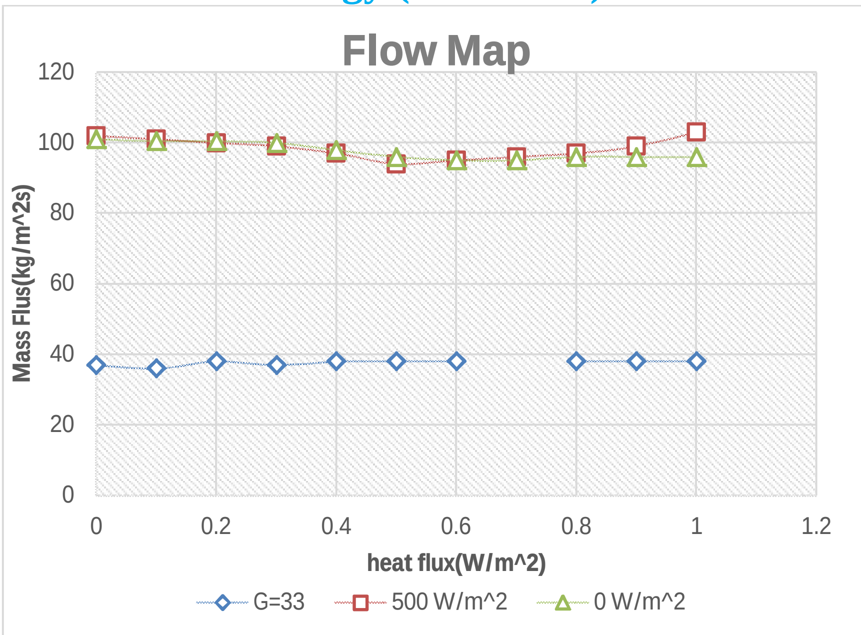

Fig .Flow map calculated at 33 kg/m²s Note that this flow map is not general for all mass fluxe

Comparison between experimental data and four different estimation methods at 31.1 kg/m²s as would be expected, the pressure drop increases with increasing mass flux. The largest pressure drop is generated downstream in t he evaporator. The reason for this is the higher vapour qualities and thus higher vapour speeds at these locations. It is interesting to n ote that the pressure drop between the relative length 0.6 and 0.8 is relatively larger (steeper curve) compared to other upstream loca tions

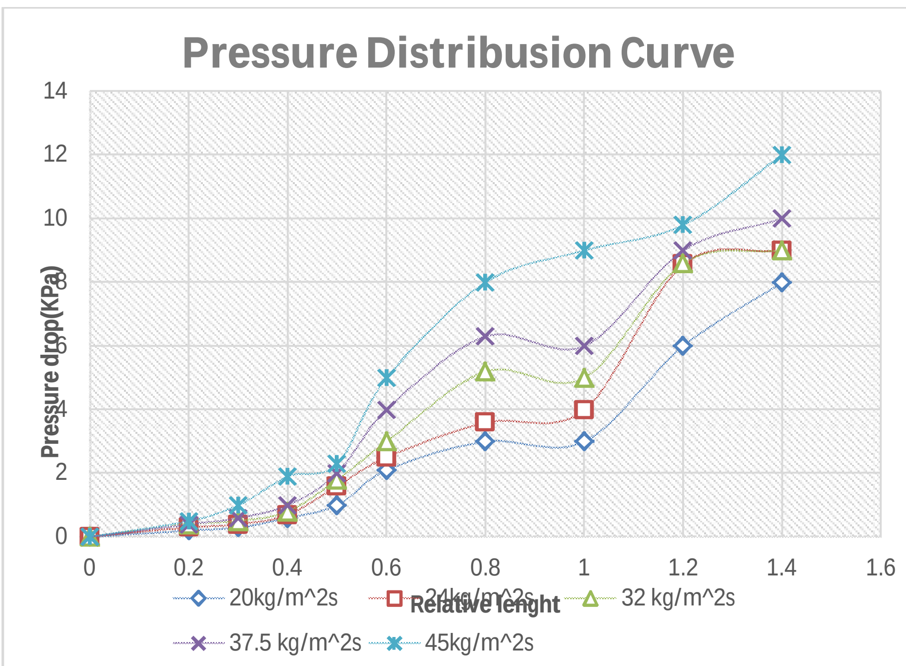

Pressure drop along the refrigerant tube at different mass fluxes

It can be seen that the experimental friction factor is well fitted with the theoretical Blasius's formula,this match was only found wh en the hydraulic diameter (3.21mm) was used, which is a good indication that the hydraulic diameter concept is applicable for the cr oss section studied.

International Journal for Research in Applied Science & Engineering Technology (IJRASET)

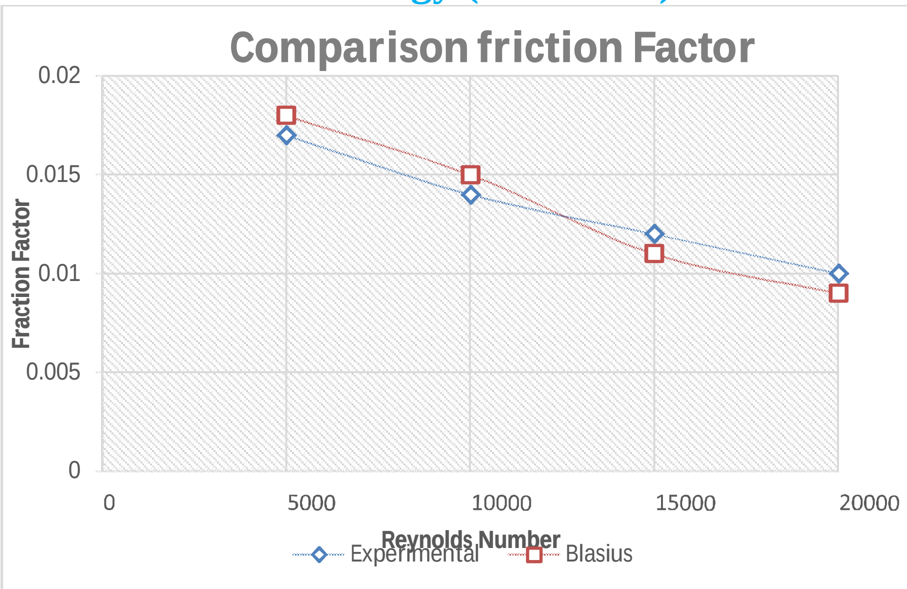

Fig .Single phase comparison of friction factor calculated by the well-known Blasius's smooth pipe formula and by the friction factor definition using experimental pressure drop data

IV. CONCLUSION

A. Correlations are suggested on how to calculate heat transfer and pressure drop in a household refrigerator evaporator.
B. A potential to increase the efficiency by about 10 % was revealed at the air side by changing the flow and radiation conditions around the evaporator.
C. Thin film evaporation at tube walls repeatedly wetted by liquid plugs was suggested to be the physical explanation to the unexpectedly high boiling heat transfer coefficients observed. This view challenges conventional in-tube evaporation knowledge.
D. A new method was developed on how to measure refrigerant charge at different locations in the cooling system.
E. Charge distribution was measured at transient and steady state conditions from which a new understanding of the system operation was achieved. Cyclic losses were estimated based upon the experimental data.
F. The subject of "throttling and charging" was systematically investigated. Results indicate insensitivity for a wide range of settings.
G. Experimental evidence suggests that the capillary tube mass flow is very sensitive to the inlet condition when the refrigerant is nearly saturated. It is sharply reduced when the sub cooling disappears and vapor enters its inlet. This effect appears to be a key mechanism for quick charge redistribution at start-up and for a stable charge distribution at varied thermal conditions.
H. A practical method on how to optimize the capillary tube length and the quantity of charge is described.
I. The cyclic losses were estimated to be 8 % (efficiency) for the studied refrigerator. In order to reduce these losses it was suggested to modify the evaporator channels into a downward inclination and to use smaller diameter at the upstream part.
J. Suggestions are made on how to increase the efficiency (1-2 %) at steady state conditions by moving the refrigerant channels closer to the evaporator edges.
K. Short cycling was found to increase the efficiency about 5 %.

REFERENCES

[1] Wang R.Z., Yu X, Ge T.S., Li T.X.. The present and future of residential refrigeration, power generation and energy storage. Applied Thermal Engineering 2012; 53: 256-70.
[2] Hassan H, Mohamad A. A review on solar cold production through absorption technology. Renewable and Sustainable Energy Reviews 2012; 16: 5331-48.
[3] Zhai X.Q., Qu M, Li Y, Wang R.Z.. A review for research and new design options of solar absorption cooling systems. Renewable and Sustainable Energy Reviews 2011; 15: 4416-23.
[4] Cabrera F, Fernández-García A, Silva R, Pérez-García M. Use of parabolic trough solar collectors for solar refrigeration and air-conditioning applications. Renewable and Sustainable Energy Reviews 2013; 20: 103-18.
[5] Eicker U, Pietruschka D. Design and performance of solar powered absorption cooling systems in office buildings. Energy and Buildings 2009; 41: 81-91.

[6] Florides GA, Kalogirou SA, Tassou S, Wrobel L. Modelling and simulation of an absorption solar cooling system for Cyprus. Solar Energy 2002; 72: 43-51.

[7] Florides GA, Kalogirou SA, Tassou S, Wrobel L. Modelling, simulation and warming impact assessment of a domesticsize absorption solar cooling system. Applied Thermal Engineering 2002; 22: 1313-25.

[8] Assilzadeh F, Kalogirou SA, Ali Y, Sopian K. Simulation and optimization of a LiBr solar absorption cooling system with evacuated tube collectors. Renewable Energy 2005; 30: 1143-59.

[9] Mazloumi M, Naghashzadegan M, Javaherdeh K. Simulation of solar lithium bromide–water absorption cooling system with parabolic trough collector. Energy Conversion and Management 2008; 49: 2820-32.

[10] Vargas J, Ordonez J, Dilay E, Parise J. Modeling, simulation and optimization of a solar collector driven water heating and absorption cooling plant. Solar Energy 2009; 83: 1232-44.

[11] Tierney MJ. Options for solar-assisted refrigeration—Trough collectors and double-effect chillers. Renewable Energy 2007; 32: 183-99.

[12] Velázquez N, García-Valladares O, Sauceda D, Beltrán R. Numerical simulation of a Linear Fresnel Reflector Concentrator used as direct generator in a Solar-GAX cycle. Energy Conversion and Management 2010; 51: 434-45.

[13] Liu Y.L., Wang R.Z.. Performance prediction of a solar/gas driving double effect LiBr–H2O absorption system. Renewable Energy 2004; 29: 1677-95. COPYRIGHT IJATSER International Journal of Advanced Technology for Science & Engineering Research. www.ijatser.com, Volume 1, Issue 4, Feb 2016 – March 2016, Page 1-6 WWW.IJATSER.COM [ALL RIGHTS RESERVED] 6

[14] Agyenim F, Knight I, Rhodes M. Design and experimental testing of the performance of an outdoor LiBr/H2O solar thermal absorption cooling system with a cold store. Solar Energy 2010; 84: 735-44.

[15] Li Z.F., Sumathy K. Experimental studies on a solar powered air conditioning system with partitioned hot water storage tank. Solar Energy 2001; 71: 285-97.

[16] Best R, Hernandez J. Experimental studies on the operating characteristics of an ammonia-water absorption system for solar cooling. Chemical engineering research & design 1991; 69: 153-60.

[17] Syed A, Izquierdo M, Rodriguez P, Maidment G, Missenden J, Lecuona A, et al. A novel experimental investigation of a solar cooling system in Madrid. International Journal of refrigeration 2005; 28: 859-71.

[18] Lizarte R, Izquierdo M, Marcos J, Palacios E. An innovative solar-driven directly air-cooled LiBr–H2O absorption chiller prototype for residential use. Energy and Buildings 2012; 47: 1-11.